1997

NASA / ASEE SUMMER FACULTY FELLOWSHIP PROGRAM

MARSHALL SPACE FLIGHT CENTER
THE UNIVERSITY OF ALABAMA IN HUNTSVILLE

UNCERTAINTY IN CALIBRATION, DETECTION, AND ESTIMATION OF METAL CONCENTRATIONS IN ENGINE PLUMES USING OPAD

Prepared by: Randall C. Hopkins / Daniel A. Benzing

Academic Rank: Instructor / Graduate Research Assistant

Institution and Department: University of Alabama - Tuscaloosa
Dept. of Aerospace Engineering and Mechanics

NASA / MSFC:

Office: Instrumentation and Control Branch
Division: Astrionics Laboratory

MSFC Colleagues: Anita Cooper
W. T. Powers
William White

Introduction

The idea of extracting chemical data from the analysis of the electromagnetic (EM) spectrum is not new. Holding a copper wire in a sufficiently hot flame produces a characteristic green region in the flame. The copper atoms are exited to such a high energy state that they emit electromagnetic radiation at several wavelengths, with green light being dominant. The atomic structure determines the wavelengths of EM emitted, and since all elements are unique, no two elements will emit EM at exactly the same wavelengths. Thus each element has its own unique spectral signature. For example, in the same flame, the element nickel will emit EM at wavelengths different than copper. A plot of radiant intensity versus wavelength is the electromagnetic spectrum of nickel, as shown in Fig. 1. Since this spectrum is unique, a spectrometric detector some distance from the flame would allow a user to determine the presence of nickel, copper, or both, in the flame.

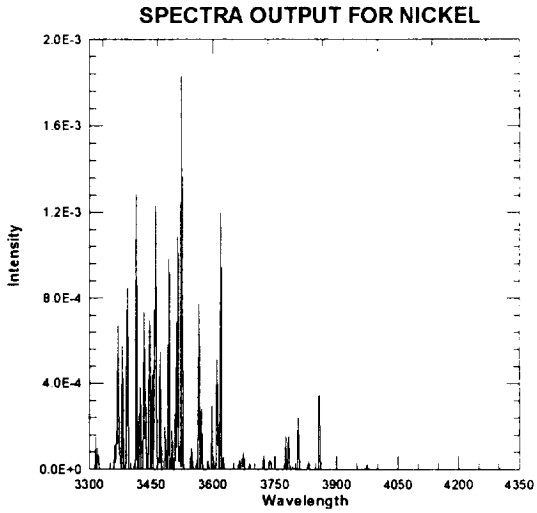

Fig. 1. Example Emission Spectra for Nickel.

Individual spectra for other elements vary in complexity, some having few atomic transitions (peaks), others having many. Three germane points of importance to this paper result from Fig. 1 and the associated radiation physics: 1) *every element has it's own "spectral signature,"* 2) *the emission will contain atomic transitions at wavelengths which may not be part of the visible spectrum, and* 3) *the* ***intensity*** *of the emission is a function of the* ***quantity*** *of emitting matter present in addition to the system temperature and other quantum variables.*

Rocket plumes are emissive events subject to the same physics (with more complications of course) as burning nickel or copper over an open flame. The Optical Plume Anomaly Detection (or OPAD) program (Cooper, *et al*, 1997) was initiated by researchers at MSFC as an effort to take advantage of the wealth of information contained in the exhaust plume of a rocket engine. The initial idea was to identify anomalous spectral events which were consistent with known mechanical failures and then use them as templates in the health monitoring of future engine tests (ground or in-flight). This could then be coupled with the anomalous events found in the vibrational and other sensor data to determine the overall state, or health, of the engine.

The "template idea," however, was soon replaced by even more ambitious goals as a result of some initial findings in the TTB experimental program (Benzing, *et al*, 1997). The spectral data from one test in particular revealed a major occurrence of a metallic species which was indigenous to the SSME

preburner faceplate. An even closer evaluation of the amount of metallic species present versus time showed an initial erosive event of the metal followed by numerous other anomalous emissions, all leading up to an engine-threatening erosion of the faceplate. This meant that anomalous events could be predicted.

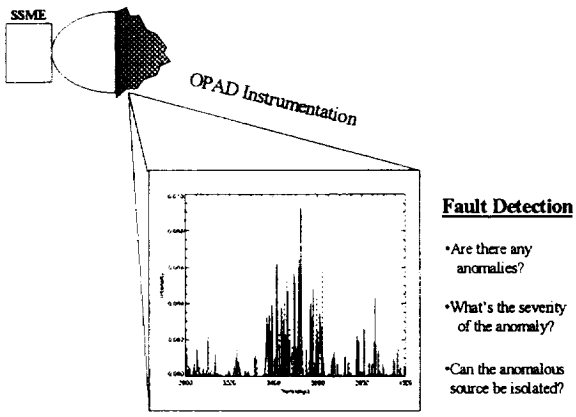

Fig. 2. Monitoring the SSME Exhaust Plume using the OPAD System.

As a result of these findings, the focus of the researchers turned to not only anomaly detection but also metal quantification. In other words, health monitoring now involved the simultaneous tasks of anomaly detection and determination of the severity of the anomaly, as illustrated in Fig. 2. This meant that the free atom densities of all the metals of interest within the engine would have to be predicted for every temporal scan taken by the instruments. The metal quantification process would essentially give metal concentration versus time. Spikes in this time trace would then be indicative of a metal erosion.

The neural network extracts radiant intensity data from the electromagnetic spectrum of the exhaust plume and uses these values to predict concentrations, as well as temperature and broadening parameter, of metals in the flame (Whitaker, *et al*, 1997). Fig. 3 illustrates the network's operation. As the intensities of the electromagnetic radiation are extracted from the spectrum, the uncertainties in those values are propagated through the network and result in uncertainties in the predictions of number density, broadening parameter, and temperature.

Calculation of the uncertainties begins with an examination of the procedure used to calibrate the instruments used in the OPAD system.

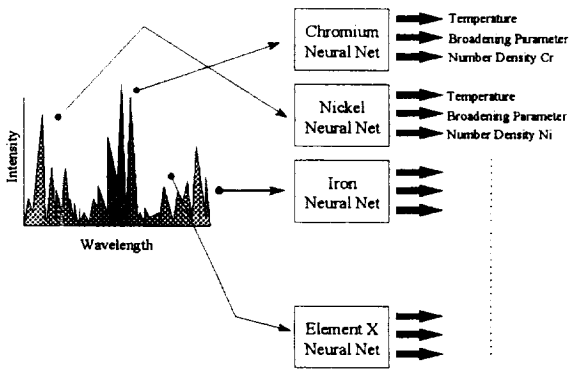

Fig. 3. Basic Operation of the Neural Network.

Uncertainties in Instrument Calibration

The purpose of instrument calibration is to determine the response of each photodetector, or the ratio of incoming radiation to outgoing voltage. During an engine test, the radiant intensity , I, at each photodetector is

$$I = (I_T - I_B) \cdot R \quad \text{(units are W/(str cm}^2\text{ ang))} \qquad (1)$$

where I_T is the radiant intensity during engine firing and I_B is the radiant intensity of the background, or ambient light. These two values are measured in "counts" since the analog-to-digital converter installed in the computer converts the voltages released by each photodetector into an integer. In order to calculate the radiant intensity, I, during the test, the value of R must be determined from calibration.

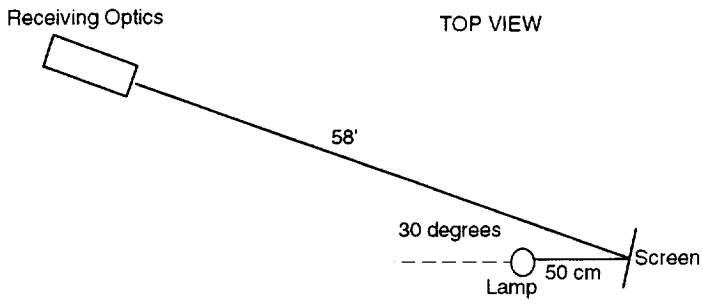

Fig. 4. Calibration Procedure for the OMA, One of Several OPAD Instruments.

Fig. 4 shows a typical calibration for the OMA, one of several spectrometers that can be used as part of the OPAD system. Using a calibrated irradiance lamp of known intensities across a segment of the electromagnetic spectrum allows the values of R in the above equation to be determined. During calibration, lamp radiation is reflected off of a screen of known reflectance properties at a certain distance from the receiving optics. Therefore, the only unknown in Equation 1 is R. Thus,

$$R(\lambda) = \frac{\left(I_{interpolated}\right)_\lambda}{\left(I_L - I_B\right)_\lambda} \tag{2}$$

where I_L is the lamp intensity (in counts) at the photodetector, and I_B is the background. Any uncertainty in R will be propagated though Equation 1 during an engine test.

Some of the sources of uncertainty in R include instrument noise, uncertainties in the lamp irradiance, uncertainties in the screen reflectance, the distance between the lamp and reflectance screen, the distance between the screen and the receiving optics, background fluctuations (such as sun and shade, time of day, changing surroundings, etc.), and others.

Due to time constraints, the uncertainty in R was determined using statistical methods. Several hundred sample calibration scans were taken at different times and the environmental factors (sun, temperature, humidity, etc.) noted. Then values of R were calculated for each photodetector for these scans. Values of R were determined by the mean of the data points and the uncertainties were reported as one standard deviation, as in Equations 3 and 4, respectively.

$$\mu = \frac{1}{n}\sum_{i=1}^{n} x_i \tag{3}$$

$$\sigma = \sqrt{\frac{1}{n-1}\sum_{i=1}^{n}(x_i - \mu)^2} \tag{4}$$

Uncertainties in the distances between the screen and lamp and the screen and the receiving optics were determined but not propagated through the calibration procedure due to time constraints; they will be included in future studies. Once these uncertainties were determined, then the uncertainties in the radiant intensity during an engine test could be determined.

Uncertainties in the Measured Photodetector Radiant Intensity

The uncertainty in I in Equation 1 can be determined mathematically using well known statistics. For each photodetector (there may be over 2000) in the instrument, the absolute uncertainty in I, expressed U_I, is

$$U_I^2 = \left[U_{I,T}\frac{\partial I}{\partial I_T}\right]^2 + \left[U_{I,B}\frac{\partial I}{\partial I_B}\right]^2 + \left[U_R\frac{\partial I}{\partial R}\right]^2 \tag{5}$$

where $U_{I,T}$ and $U_{I,B}$ are the uncertainties in the measured exhaust plume and background (pre-test) radiance, and U_R is the uncertainty in the photodetector response. Evaluating the partial derivatives results in a simple expression:

$$(U_I)^2 = (U_{I,T}R)^2 + (U_{I,B}R)^2 + (U_R(I_T - I_B))^2 \tag{6}$$

Use of Equation 6 allows one to not only evaluate the overall uncertainty, but also determine the major contributors. This shows the experimenter what areas of the experiment should be improved.

To evaluate these equations by hand would be extremely time consuming for experiments of several hundred scans using instruments of over 2000 photodetectors. Therefore, five ANSI standard C programs were written to convert raw data from the instruments a standard format, analyze the data for entire scans or for individual photodetectors, create histograms and temporal charts, and compute the mean, standard deviation, and absolute and relative uncertainties in any measurement, whether it be counts (such as I) or values of R. These programs can average several background scans, or randomly mix background (I_B) and calibration (I_L) or engine test (I_T) scans. The results of these programs are then substituted into Equation 6.

Analysis of each term for photodetector number 099 of the OMA instrument is shown in Table 1.

$$(U_I) = 7.501E-08 \frac{W}{str \cdot cm^2 \cdot ang}$$

$$\left(U_{I,T} R\right)^2 = 1.198E-16$$

$$\left(U_{I,B} R\right)^2 = 7.862E-18$$

$$\left(U_R (I_T - I_B)\right)^2 = 1.170E-15$$

Table 1. Contributions to the Uncertainty for Photodetector #99 in the OMA Instrument.

The data used in the analysis in Table 1 are from an SSME test. The results clearly show that the uncertainty (expressed as 1σ) in background measurements contribute the least to the overall uncertainty. However, for photodetector number 99, U_R is 3.641E-10 (4.802%), and in the third term U_R is multiplied by a large number (I_T - I_B = 1030 counts on average). Thus if the exhaust plume is extremely bright, then this error term dominates, and the errors during the calibration process become very important.

Propagation Through the Neural Network

The neural network takes the intensity values from Equation 1 and predicts temperature, number density, and broadening parameter for the flow. What can be said of the uncertainties in these estimates? Generally speaking there are three main sources of uncertainty in the radial basis function neural network (RBFNN) estimation: 1) error due to the inability of the neural model to completely map the underlying physical relationship, 2) uncertainty in the training data as a result of the *Spectra6** models' inability to completely describe the physical nature of the flow emission, and 3) uncertainties introduced during the calibration/response function creation processes.

Typically, the statement of uncertainties in a neural network prediction involve only error estimates that are based on the neural model's inability to fit the training data. No consideration is given to the error component introduced through the acquisition of the actual testing or training data sets. The terse technical note described herein serves to highlight this error component and provide a means by which its effects can be quantified.

The general architecture of the RBFNN is given in Fig. 5 below. It is assumed that prior knowledge of the uncertainties in the inputs has been established. The figure shows a fully connected RBF network with radial kernels and associated weighting factors. The kernel function can be any radially symmetric function; that is, a function which has a "local" behavior such as the Gaussian, Cauchy, or Multiquadric. The output quantities (y_k) are then given by the basis function expansion of Equation 7.

$$y_k = \sum_{j=1}^{m} w_{jk}(g_j) \qquad (7)$$

* The *Spectra6* model is a computer program that produces the training data for the RBFNN. Inputs into the program are quantum variables; outputs are an electromagnetic spectrum and associated temperature, number density, and broadening parameter. (Cooper, *et al*, 1997)

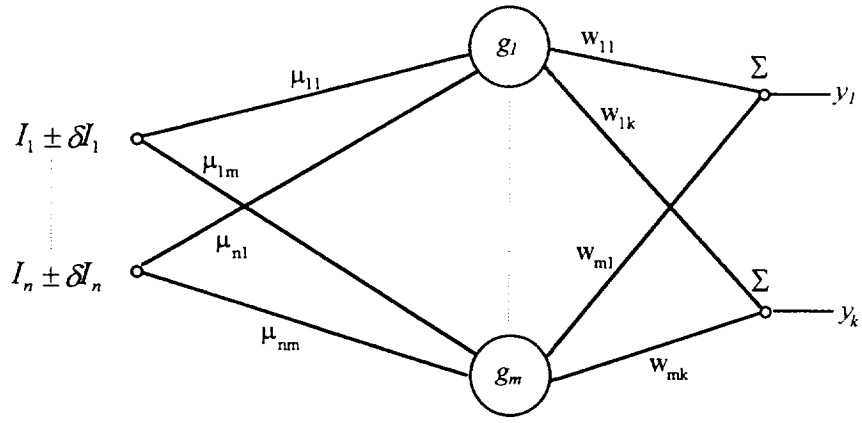

Fig. 5. RBFNN General Architecture.

Note, the bias term in Equation 7 is not included because it drops out in the partial derivative expansion. For the sake of analysis, assume the kernel function is a Gaussian (Equation 8) and that the network coefficients (w_{ii}, μ_{ii}) have already been established. Further assume that any uncertainties associated with the network inputs are independent and random. With these conditions, the uncertainty in an output variable can be obtained via Equation 9 below.

$$g_m = \exp\left\{-\frac{\sum_{i=1}^{n}(I_i - \mu_{mi})^2}{R^2}\right\} \tag{8}$$

$$(\delta y_k)^2 = \sum_{i=1}^{n}\left(\delta I_i \frac{\partial y_k}{\partial I_i}\right)^2 \tag{9}$$

Through a trivial (just kidding) partial expansion, the partial derivatives can be evaluated as,

$$\frac{\partial y_k}{\partial I_n} = \sum_{j=1}^{m} w_{jk} \frac{\partial g_j}{\partial I_n} \tag{10}$$

As an example, the paritial expansion has been worked out for the Gaussian kernel below,

$$\frac{\partial y_k}{\partial I_n} = \sum_{j=1}^{m} w_{jk} g_j \bullet \left(-\frac{2}{R^2}(I_n - \mu_{jn})\right) \tag{11}$$

Conclusions

Improvements in uncertainties in the values of radiant intensity (I) can be accomplished mainly by improvements in the calibration process and in minimizing the difference between the background and engine plume radiance. For engine tests in which the plume is extremely bright, the difference in luminance between the calibration lamp and the engine plume radiance can be so large as to cause relatively large uncertainties in the values of R. This is due to the small aperture necessary on the receiving optics to avoid saturating the instrument. However, this is not a problem with the SSME engine since the liquid oxygen / hydrogen combustion is not as bright as some other fuels. Applying the instrumentation to other type engine tests may require a much brighter calibration lamp.

References

Cooper, A.E., Powers, W.T., Wallace, T.L., Buntine, W., "Recent Results in the Analysis of Large Rocket Engine anomalies Utilizing State-of-the-Art Spectral Modeling Algorithms," 1997 JANNAF.

Benzing, Daniel A., Hopkins, Randall C., Whitaker, Kevin W., "OPAD: An Innovative Rocket Engine Health Monitoring System," *Proceedings of the 16th Annual Digital Avionics System Conference*, 1997.

Whitaker, K L., Moore, D., Benzing, D.A., "A Neural Network Approach to Anomaly Detection in Spectra," *35th Aerospace Sciences Meeting & Exhibit*, AIAA-97-0223, Reno, NV, 1997